Journal of Nano- and Electronic Physics
Vol. **18** No 3, 03030(8pp) (2026)

Журнал нано- та електронної фізики
Том **18** № 3, 03030(8cc) (2026)

OPEN ACCESS

REGULAR ARTICLE

Optical Antenna-Resonator Based on a Metallic Prolate Spheroidal Nanoparticle

A.V. Korotun[1,2,*], V.P. Kurbatsky[1], H.V. Moroz[1], R.Yu. Korolkov[1], N.M. Nagorna[1]

[1] *Zaporizhzhia Polytechnic National University, 69063 Zaporizhzhia, Ukraine*
[2] *G.V. Kurdyumov Institute for Metal Physics, N.A.S. of Ukraine, 03142 Kyiv, Ukraine*

(Received 20 March 2026; revised manuscript received 14 June 2026; published online 26 June 2026)

The antenna and resonator characteristics of prolate spheroidal metallic nanoparticles are investigated. The operating principle of an optical nanoscale antenna is discussed. The relationship between the antenna and resonator properties of metallic nanoparticles is established. The frequency and size dependences of the field longitudinal enhancement, quality factor, Purcell factor, and spontaneous emission-resonator coupling factor are obtained, as well as the size dependences of the lightning rod coefficient, efficiency, longitudinal surface plasmon resonance frequency, and spontaneous emission rate change. Relationships are established linking these quantities, which indicate a close relation between the characteristics of nanoscale optical antennas and nanoresonators. The behavior of the maxima in the frequency dependences of the field longitudinal enhancement and Purcell factor with varying eccentricity of a spheroidal nanoparticle is described. It is shown that with increasing particle eccentricity (approaching a cylindrical shape), the lightning rod coefficient, efficiency, and spontaneous emission rate change increase. At the same time, the longitudinal surface plasmon resonance frequency decreases, moving from the near ultraviolet to the optical (for particles of some metals – to the infrared) range. It is established that in the limiting case of a particle of infinite length, the lightning rod coefficient becomes infinitely large. A close relationship was discovered between the antenna and resonator properties of spheroidal nanoparticles, confirmed by the spontaneous emission-resonator coupling factor being close to unity in the infrared and visible spectral regions. It is established that an increase in the surface area-to-volume ratio of nanoparticles with a decrease in their size leads to a decrease in the efficiency and an increase in the spontaneous emission rate change. In addition, with an increase in the size (lengths of the semi-axes) of nanoparticles, an increase in the longitudinal component of the quality factor tensor is observed.

Keywords: Optical nanoantenna, Nanoresonator, Lightning rod coefficient and efficiency, Electric field amplification, Quality factor, Purcell factor.

DOI: 10.21272/jnep.18(3).03030 PACS numbers: 42.60.By, 73.20.Mf, 84.40.Ba

1. INTRODUCTION

Optical radiation control is a fundamental component of modern technologies, encompassing lighting, visualization, sensorics, detection, storage and processing of information, and energy management systems. Various optical elements – from light sources to focusing and shaping components – are widely used in applied and fundamental research in medicine, biology, chemistry, and materials science [1-4]. Classical optical devices are based on well-known physical principles – reflection, refraction, interference and diffraction – which enable modification of the light front structure and control of the electromagnetic wave propagation direction on a macroscopic scale [5].

Despite significant progress achieved in macroscopic optical modeling, precise control of light at subwavelength scales remains a challenging task [6]. The main difficulty is related to diffraction limitations, due to which the minimum size of optical elements is equal in order of magnitude to the wavelength. This hinders the direct observation and control of nanoscale objects – organic molecules, nanoparticles, nanostructured surfaces, and functional elements of nanophotonic devices [7, 8]. In this regard, the development of new methods for subwavelength light manipulation is a current trend in modern optics and nanophotonics.

Nanoparticles play a leading role in overcoming the diffraction limit; their special optical properties enable the transition from macroscopic to nanoscale effects [9]. Concepts used in classical radiofrequency antennas have been scaled up to the nanoscale, that made it possible to form a new class of optical nanoantennas. One of the most well-known prototypes is a structure similar to the Yagi-Uda antenna [10], which includes a reflector, an active element, and a system of directors that provide phase matching and interference of reradiated waves in a selected direction. The Yagi-Uda nanoantenna, modified for the optical range, demonstrates the ability to directionally emit and convert light with high angular contrast at the [11, 12].

In recent years, methods for controlling directional scattering and radiation have evolved significantly. A wide range of nanostructures capable of generating asymmetric scattering patterns and providing highly precise energy redirection have been formed. An im-

* Correspondence e-mail: andko@zp.edu.ua

Cite this article as: A.V. Korotun et al., *J. Nano- Electron. Phys.* 18 No 3, 03030 (2026) https://doi.org/10.21272/jnep.18(3).03030

portant place among these is occupied by metallic nanostructures, the optical properties of which are determined by localized surface plasmon resonances [1-4, 13]. Such resonances are associated with collective oscillations of electrons within metallic nanoparticles and can be qualitatively described by an equivalent LRC model [14], which takes into account the inductive, resistive, and capacitive contributions of the material and its environment. The significant enhancement of the local electric field and large optical cross section make plasmonic nanoparticles key elements in photocatalysis [15, 16], sensor technologies [17], photovoltaics [18, 19] and nonlinear optics [20].

The superposition of dipole and multipole plasmonic modes determines the nature of the optical nanoantenna's directivity and thus allows the formation of resonant structures with specified spectral and spatial characteristics. The features of resonant interaction and directional scattering have provided nanoantennas with a wide range of applications [21-24]. In particular, optical nanoantennas are used for spectral-spatial routing of light with simultaneous separation of radiation by frequency and direction in multichannel optical communication systems [24]. Such structures are effective in chemical and biomedical sensors, where local amplification of the electromagnetic field increases sensitivity to changes in the refractive index of the medium under study. The interaction of nanoantennas with fluorescent emitters and molecules capable of Raman scattering significantly increases the detection efficiency and allows observation at the level of individual molecules [25].

Thus, directional optical nanoantennas represent a versatile nanophotonics tool, suitable for a wide range of applications, from highly informative spectroscopy and biosensors to optical routing and energy conversion. An ability to provide diffraction limitation-free control of light determines the importance of their further research.

The development of nanotechnology has led to the creation of yet another type of optical device – nanoresonators with a giant Q factor. A number of studies published over the past two decades [21, 26] have established that, for subwavelength resonator dimensions, their differences from optical nanoantennas become negligible. Therefore, despite significant losses in metals, there is a real possibility of optical antennas functioning as nanoscale resonators with a controlled Q factor [27]. It should be noted that the resonator properties of spherical metal nanoparticles were considered in [28], and the antenna and resonator properties of nanoparticles of other shapes were investigated in [26]. The question of the relation between antenna and resonator characteristics remains open, and establishing this relationship for metal nanoparticles in the shape of a prolate spheroid is a current problem.

2. PHYSICAL AND TECHNICAL CHARACTERISTICS OF OPTICAL NANO-SCALE ANTENNAS AND RESONATORS

2.1 Operating Principle of an Optical Nanoantenna

The most important characteristic of an antenna is its directivity. It determines the degree of concentration of radiation in one direction. Generally, the directivity of an antenna is equal to the ratio of the energy flow in the direction of maximum radiation to the energy flow averaged over all directions.

It is known that a single dipole or quadrupole source is unable to create a narrowly directed scattering, since both resonant modes have mirror symmetry in the plane of the electric field $\mathscr{E}$ and the wave vector $\boldsymbol{k}$. To maintain directional scattering, mirror symmetry in the resonant regime must be eliminated. For this reason, nanoparticle antennas, as the simplest type of antennas, have a *V*-shape [29], the shape of triangular nanoplates [30], nanorods [24, 31], prolate nanospheroids and nanorods on a substrate [32]. The directivity of light scattering arises as a result of constructive and destructive interference of different plasmonic modes.

To measure the directivity of light scattered by nanoparticle-antennas, back-focal plane (BFP) imaging is used [29, 30]. The setup for BFP imaging is shown in Fig. 1. Light coming from the sample plane is a superposition of plane waves with different wave vectors. These components are separated by a lens. After passing through the lens, beams with identical wave vectors are focused at a specific point in the BFP, forming an $\boldsymbol{k}$-image of the light flux scattered by the nanoparticle-antenna.

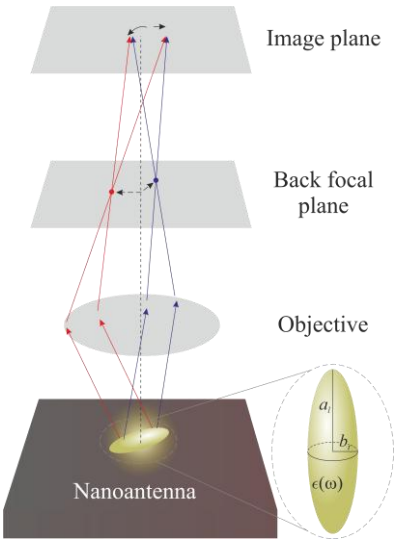

Fig. 1 – Schematic of the BFP imaging setup. Blue and red arrows represent light from the nanoantenna scattered in two different directions. The dotted line denotes the optical axis of the setup

In addition to exploiting the interference between dipole and quadrupole plasmonic modes, proper placement of dipoles also enables directional scattering. Axisymmetric metal nanoparticles located on a silicon substrate produce scattering over a broad spectral range [31]. Since the silicon substrate has a high refractive index, the longitudinal plasmonic modes of the metal nanospheroid are suppressed by the image charges in the substrate. Oscillating charges on the nanoparticle surface and image charges in the substrate form a series of nearby dipole

sources. The dipoles are oriented perpendicular to the long axis and to the substrate surface. Therefore, a metal nanoparticle located on a silicon substrate can be considered as an array of vertically oriented dipoles. The light from the ED array oscillating in phase is scattered into two sides of the array. The characteristics of such a nanoantenna are determined mainly by its length and the refractive index of the substrate.

2.2 Basic Relationships

Let a metal nanoparticle have the shape of a prolate spheroid with major a_l and minor b_t semi-axes and be embedded in a dielectric with permittivity $\epsilon_{\rm m}$ (Fig. 1). The optical characteristics of a particle of this geometry (field enhancement, quality factor, polarizability, and permittivity) are second-rank diagonal tensors. Only the longitudinal components of these tensors will be used later.

Let us begin the analysis of antenna and resonator characteristics of prolate spheroidal metal nanoparticles with expressions for the longitudinal component of the electric field local enhancement tensor

$$\mathcal{F}_{\parallel}(\omega)=\left|\frac{\epsilon_{\parallel}(\omega)}{\mathcal{L}_{\parallel}\epsilon_{\parallel}(\omega)+(1-\mathcal{L}_{\parallel})\epsilon_{\rm m}}\right|^2, \tag{1}$$

$$\mathcal{F}_{\parallel}(\omega)=\left|1+2\zeta\frac{\alpha_{\parallel}(\omega)}{a^3}\right|^2, \tag{2}$$

where ζ is the lightning rod coefficient; $\mathcal{L}_{\parallel}$ is the depolarization factor of a prolate spheroid, equal to

$$\mathcal{L}_{\parallel}=\frac{1-e_p^2}{e_p^2}\left(-1+\frac{1}{2e_p}\ln\frac{1+e_p}{1-e_p}\right), \tag{3}$$

$e_p=\sqrt{1-b_t^2/a_l^2}$ is the eccentricity of the spheroid; the longitudinal component of polarizability is equal to

$$\alpha_{\parallel}(\omega)=V\frac{\epsilon_{\parallel}(\omega)-\epsilon_{\rm m}}{\epsilon_{\rm m}+\mathcal{L}_{\parallel}\left[\epsilon_{\parallel}(\omega)-\epsilon_{\rm m}\right]}, \tag{4}$$

$V=4\pi a_l b_t^2/3$ is the volume of the nanoparticle. The longitudinal component of the dielectric tensor within the Drude model is determined by the expression

$$\epsilon_{\parallel}(\omega)=\epsilon^{\infty}-\frac{\omega_p^2}{\omega\left(\omega+{\rm i}\,\gamma_{\rm eff}^{\parallel}\right)}. \tag{5}$$

In formula (5), ϵ^{∞} is the contribution of the ionic subsystem to the permittivity; ω_p is the plasma frequency. The longitudinal effective relaxation rate has the form

$$\gamma_{\rm eff}^{\parallel}=\gamma_{\rm bulk}+\gamma_{\rm s}^{\parallel}+\gamma_{\rm rad}^{\parallel}, \tag{6}$$

where the volume relaxation rate $\gamma_{\rm bulk}=\text{const}$, longitudinal rates of surface relaxation and radiative attenuation are respectively equal to [32]

$$\gamma_{\rm s}^{\parallel}=\frac{9}{16}\frac{\mathcal{L}_{\parallel}}{\epsilon_{\rm m}+\mathcal{L}_{\parallel}(1-\epsilon_{\rm m})}\left(\frac{\omega_p}{\omega}\right)^2\frac{v_{\rm F}}{2b}\mathcal{F}_{\parallel}(e_p), \tag{7}$$

$$\gamma_{\rm rad}^{\parallel}=\frac{V}{8\pi}\frac{\mathcal{L}_{\parallel}}{\sqrt{\epsilon_{\rm m}\left(\epsilon^{\infty}+\dfrac{1-\mathcal{L}_{\parallel}}{\mathcal{L}_{\parallel}}\epsilon_{\rm m}\right)}}\left(\frac{\omega_p}{c}\right)^3\left(\frac{\omega_p}{\omega}\right)^2\frac{v_{\rm F}}{2b}\mathcal{F}_{\parallel}(e_p). \tag{8}$$

In expressions (7) and (8), $v_{\rm F}$ is the Fermi velocity of electrons,

$$\mathcal{F}_{\parallel}(e_p)=\frac{1}{e_p^3}\left\{\frac{\pi}{2}-\arcsin\sqrt{1-e_p^2}+e_p\sqrt{1-e_p^2}\left(2e_p^2-1\right)\right\}. \tag{9}$$

Currently, the opinion has become established among researchers that nanoscale metal antennas can be considered as nanoresonators [26]. Let us establish a connection between the characteristics of antennas and the parameters of optical nanoresonators.

2.3 Lightning Rod Coefficient, Efficiency and Spontaneous Emission Rate Change

By equating expressions (1) and (2) and taking into account relation (4), we obtain the size dependence of the lightning rod coefficient

$$\zeta(e_p)=\frac{3\left(1-\mathcal{L}_{\parallel}(e_p)\right)}{8\pi\left(1-e_p^2\right)}. \tag{10}$$

In antenna theory, efficiency is the ratio of the radiated power to the power transmitted from the load to the antenna. For emitters-nanoparticles, efficiency is determined by the rates of surface relaxation and radiative attenuation [21]:

$$\eta_a=\left(1+\frac{\gamma_{\rm s}^{\parallel}}{\gamma_{\rm rad}^{\parallel}}\right)^{-1}. \tag{11}$$

Using formulas (7) and (8), we obtain expressions for the efficiency

$$\eta_a=\left\{1+\frac{27}{8\left(1-e_p^2\right)}\left(\frac{c}{\omega_p a}\right)^3\frac{\sqrt{\epsilon_{\rm m}\left(\epsilon^{\infty}+\dfrac{1-\mathcal{L}_{\parallel}(e_p)}{\mathcal{L}_{\parallel}(e_p)}\epsilon_{\rm m}\right)}}{\left[\epsilon_{\rm m}+(1-\epsilon_{\rm m})\mathcal{L}_{\parallel}(e_p)\right]}\right\}^{-1} \tag{12}$$

and the spontaneous emission rate change

$$w=\frac{\mathcal{F}_{\parallel}}{\eta_a}. \tag{13}$$

Formula (13) represents the relationship between the important characteristics of the nanoantenna – the spontaneous emission rate change, efficiency and the electric field enhancement.

2.4 Quality Factor of Optical Resonators

The quality factor of nanoscale resonators is analogous to the Q factor of an optical antenna and is determined by the expression [34]

$$Q_{\parallel} = \frac{\omega}{2\,\mathrm{Im}\,\epsilon^{\parallel}(\omega)} \frac{d}{d\omega}\left[\mathrm{Re}\,\epsilon^{\parallel}(\omega)\right]. \tag{14}$$

Since inequality $\gamma_{\mathrm{eff}}^{\parallel} \ll \omega$ is satisfied in the working spectral range of the optical nanoscale antenna, from (14) taking into account formula (5) we can obtain

$$Q_{\parallel} = \frac{\omega_p^2}{\omega\gamma_{\mathrm{eff}}^{\parallel}(\omega)}. \tag{15}$$

At $\omega = \omega_{sp}^{\parallel}$ we have the size dependence of the longitudinal quality factor in the form

$$Q_{\parallel}(e_p) = \frac{\omega_p^2}{\omega_{sp}^{\parallel}(e_p)\gamma_{\mathrm{eff}}^{\parallel}\left[\omega_{sp}^{\parallel}(e_p)\right]}, \tag{16}$$

where the longitudinal effective relaxation rate is determined by the expression

$$\gamma_{\mathrm{eff}}^{\parallel}\left(\omega_{sp}^{\parallel}\right) = \frac{\mathcal{L}_{\parallel}(e_p)}{8}\frac{v_{\mathrm{F}}}{2b}\left(\frac{\omega_p}{\omega_{sp}^{\parallel}(e_p)}\right)^2\left\{\frac{9}{2}\frac{1}{\epsilon_{\mathrm{m}}+\mathcal{L}_{\parallel}(e_p)(1-\epsilon_{\mathrm{m}})}+\frac{V}{\pi}\left[\epsilon_{\mathrm{m}}\left(\epsilon^{\infty}+\frac{1-\mathcal{L}_{\parallel}(e_p)}{\mathcal{L}_{\parallel}(e_p)}\epsilon_{\mathrm{m}}\right)\right]^{-1/2}\left(\frac{\omega_p}{c}\right)^3\right\}\mathcal{F}_{\parallel}(e_p)+\gamma_{\mathrm{bulk}}. \tag{17}$$

The frequency of longitudinal surface plasmon resonance (at $\gamma_{\mathrm{eff}}^{\parallel} \to 0$) is equal to

$$\omega_{sp}^{\parallel} = \frac{\omega_p}{\sqrt{\epsilon^{\infty}+\dfrac{1-\mathcal{L}_{\parallel}}{\mathcal{L}_{\parallel}}\epsilon_{\mathrm{m}}}}. \tag{18}$$

Let us move on to finding the relationships between the antenna and resonator characteristics of an prolate spheroidal metal nanoparticle.

2.5 Relations Between the Characteristics of Optical Nanoscale Antennas and Nanoresonators

Substituting expression (5) into formula (1), after a series of transformations, we obtain an expression for the size dependence of the electric field longitudinal enhancement

$$\mathcal{F}_{\parallel}(e_p) = \frac{1}{\mathcal{L}_{\parallel}^2(e_p)}\left[1+\left(1-\mathcal{L}_{\parallel}(e_p)\right)^2\epsilon_{\mathrm{m}}^2\frac{\omega_{sp}^{\parallel\,6}(e_p)}{\omega_p^4\gamma_{\mathrm{eff}}^{\parallel\,2}\left[\omega_{sp}^{\parallel}(e_p)\right]}\right]. \tag{19}$$

Combining relations (16) and (19), we find the relationship between the field enhancement (antenna characteristic) and the quality factor (resonator characteristic)

$$\mathcal{F}_{\parallel} = \frac{1}{\mathcal{L}_{\parallel}^2}\left[1+\frac{\left(1-\mathcal{L}_{\parallel}\right)^2\epsilon_{\mathrm{m}}^2}{\left(\epsilon^{\infty}+\dfrac{1-\mathcal{L}_{\parallel}}{\mathcal{L}_{\parallel}}\epsilon_{\mathrm{m}}\right)^2}Q_{\parallel}^2\right]. \tag{20}$$

By analogy with formulas (19) and (20), we obtain expressions for the size dependence of the spontaneous emission rate change

$$w(e_p) = \frac{1}{\mathcal{L}_{\parallel}^2(e_p)}\left[1+\left(1-\mathcal{L}_{\parallel}(e_p)\right)^2\epsilon_{\mathrm{m}}^2\frac{\omega_{sp}^{\parallel\,6}(e_p)}{\omega_p^4\gamma_{\mathrm{eff}}^{\parallel\,2}\left[\omega_{sp}^{\parallel}(e_p)\right]}\right]\left[1+\frac{27}{8\left(1-e_p^2\right)}\frac{\sqrt{\epsilon^{\infty}+\dfrac{1-\mathcal{L}_{\parallel}(e_p)}{\mathcal{L}_{\parallel}(e_p)}\epsilon_{\mathrm{m}}}}{\epsilon_{\mathrm{m}}+\left(1-\epsilon_{\mathrm{m}}\right)\mathcal{L}_{\parallel}(e_p)}\left(\frac{c}{\omega_p a}\right)^3\right] \tag{21}$$

and the dependence of the spontaneous emission rate change on the quality factor

$$w = \frac{1}{\mathcal{L}_{\parallel}^2}\left[1+\frac{\left(1-\mathcal{L}_{\parallel}\right)^2\epsilon_{\mathrm{m}}}{\left(\epsilon^{\infty}+\dfrac{1-\mathcal{L}_{\parallel}}{\mathcal{L}_{\parallel}}\epsilon_{\mathrm{m}}\right)^2}Q_{\parallel}^2\right]\left[1+\frac{27}{8\left(1-e_p^2\right)}\frac{\sqrt{\epsilon^{\infty}+\dfrac{1-\mathcal{L}_{\parallel}}{\mathcal{L}_{\parallel}}\epsilon_{\mathrm{m}}}}{\epsilon_{\mathrm{m}}+\left(1-\epsilon_{\mathrm{m}}\right)\mathcal{L}_{\parallel}}\left(\frac{c}{\omega_p a}\right)^3\right]. \tag{22}$$

2.6 Longitudinal Purcell Factor and Spontaneous Emission-Resonator Coupling Factor

Important characteristics describing the optical properties of a system consisting of a prolate spheroidal metal nanoparticle-resonator and a dipole molecule (Fig. 2) are the Purcell factor and spontaneous emission- resonator coupling factor, determined by the relations [28]

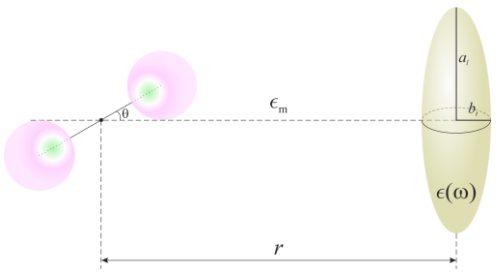

Fig. 2 – Dipole in the vicinity of an prolate spheroidal nanoparticle

$$\mathcal{F}_p^{\parallel}=\frac{8\pi^4c^3\omega_{sp}^{\parallel}}{Q_{\parallel}V_{sp}^{\parallel}\omega^2\left[\left(\omega-\omega_{sp}^{\parallel}\right)^2+\left(\omega_{sp}^{\parallel}/Q_{\parallel}\right)^2\right]}\left(1+\frac{1+3\cos^2\theta}{\epsilon_{\mathrm{m}}^2}\frac{a^2b^4}{r^6}\left|\tilde{\alpha}_{\parallel}\right|^2\right), \tag{23}$$

$$\beta_{\parallel}(\omega)=\frac{\mathcal{F}_p^{\parallel}(\omega)}{1+\mathcal{F}_p^{\parallel}(\omega)}, \tag{24}$$

where θ is the angle between the dipole and the line connecting it with the center of the nanoparticle; r is the distance from the dipole to the center of the particle;

$$\left|\tilde{\alpha}_{\parallel}\right|^2=\frac{\left|\alpha_{\parallel}\right|^2}{V^2}$$

is the square of the dimensionless polarizability. The volume of the longitudinal plasmon mode is determined by the expression

$$V_{sp}^{\parallel}=\left(\frac{\pi c}{\omega_{sp}^{\parallel}\sqrt{\epsilon_{\mathrm{m}}}}\right)^3. \tag{25}$$

Now we obtain expressions for the size dependences of the Purcell factor and the coupling factor of spontaneous emission with the nanoparticle-resonator at the longitudinal surface plasmon resonance frequency (at $\omega=\omega_{sp}^{\parallel}$). In this case

$$\left|\mathrm{Re}\,\epsilon_{\parallel}\left(\omega_{sp}^{\parallel}\right)\right|\gg\mathrm{Im}\,\epsilon_{\parallel}\left(\omega_{sp}^{\parallel}\right), \tag{26}$$

and from relation (5) we find that

$$\begin{aligned}\mathrm{Re}\,\epsilon_{\parallel}\left(\omega_{sp}^{\parallel}\right)&=-\frac{1-\mathcal{L}_{\parallel}}{\mathcal{L}_{\parallel}}\epsilon_{\mathrm{m}};\\ \mathrm{Im}\,\epsilon_{\parallel}\left(\omega_{sp}^{\parallel}\right)&\cong\frac{\omega_p^2\gamma_{\mathrm{eff}}^{\parallel}\left[\omega_{sp}^{\parallel}\left(e_p\right)\right]}{\omega_{sp}^{\parallel\,3}\left(e_p\right)},\end{aligned} \tag{27}$$

The expression for the square of the modulus of dimensionless longitudinal polarizability takes the form

$$\left|\tilde{\alpha}_{\parallel}\right|^2\cong1+\left(\frac{3\epsilon_{\mathrm{m}}\omega_{sp}^{\parallel\,3}\left(e_p\right)}{\omega_p^2\gamma_{\mathrm{eff}}^{\parallel}\left[\omega_{sp}^{\parallel\,3}\left(e_p\right)\right]}\right)^2. \tag{28}$$

Substituting expressions (16) and (28) into formula (23), we obtain

$$\mathcal{F}_p^{\parallel}\left(e_p\right)=\frac{8\pi^4\epsilon_{\mathrm{m}}^{3/2}\omega_{sp}^{\parallel}\left(e_p\right)}{\gamma_{\mathrm{eff}}^{\parallel}\left[\omega_{sp}^{\parallel\,3}\left(e_p\right)\right]}\left\{1+\frac{1+3\cos^2\theta}{\epsilon_{\mathrm{m}}^2}\frac{a^2b^4}{r^6}\left[1+\left(\frac{3\epsilon_{\mathrm{m}}\omega_{sp}^{\parallel\,3}\left(e_p\right)}{\omega_p^2\gamma_{\mathrm{eff}}^{\parallel}\left[\omega_{sp}^{\parallel\,3}\left(e_p\right)\right]}\right)^2\right]\right\}. \tag{29}$$

In the following, to obtain numerical results, formulas (1), (10), (12), (14), (16), (18), (19), (21), (23), (24), (29) were used, taking into account relations (3) and (17).

3. CALCULATION RESULTS AND DISCUSSION

Calculations of the frequency and size dependences for the longitudinal components of the field enhancement, the quality factor, the Purcell factor (at $\theta=0^{\circ}$), and the spontaneous emission-resonator coupling factor, as well as the size dependences of the lightning rod coefficient, efficiency, the spontaneous emission rate change, and the longitudinal surface plasmon resonance frequency, were performed for prolate spheroidal Ag nanoparticles. The parameters required for the calculations are listed in Table 1.

Table 1 – The parameters of metals [33, 34].

Metals	Value			
	ϵ^{∞}	$v_{\mathrm{F}}, 10^6$ m/s	$\hbar\omega_p$, eV	$\hbar\gamma_{\mathrm{bulk}}$, eV
Ag	3.7	1.45	9.17	0.016

Figure 3 shows the frequency and size dependences of the longitudinal component of the electric field enhancement tensor. The frequency dependence curves demonstrate a red shift of $\max\left\{\mathcal{F}_{\parallel}\right\}$ and an increase in the amplitude of these maxima with increasing spheroid eccentricity. This fact is confirmed by the size dependence curves of the longitudinal enhancement, which show a nonlinear increase in enhancement with increasing eccentricity. This behavior of the longitudinal field enhancement can be explained by the fact that with increasing eccentricity, the shape of the nanoparticle evolves from spherical ($e_p=0$) to cylindrical ($e_p\simeq1$).

Table 2 – Lightning rod coefficient, longitudinal surface plasmon resonance frequency and spontaneous emission- resonator coupling factor at different eccentricity values.

e_p	ζ	$\hbar\omega_{sp}^{\parallel}$, eV	$\beta_{\parallel}$
0.05	0.080	3.180	0.999
0.10	0.081	3.176	0.999
0.15	0.082	3.169	0.999
0.20	0.084	3.160	0.999
0.25	0.086	3.147	0.999
0.30	0.089	3.131	0.999
0.35	0.093	3.112	0.999
0.40	0.098	3.088	0.999
0.45	0.104	3.060	0.999
0.50	0.112	3.026	0.999
0.55	0.122	2.986	0.999
0.60	0.135	2.938	1.0
0.65	0.152	2.880	1.0
0.70	0.176	2.809	1.0
0.75	0.210	2.721	1.0
0.80	0.262	2.608	1.0
0.85	0.51	2.456	1.0
0.90	0.535	2.235	1.0
0.95	1.102	1.858	1.0

Table 2 shows the values of the lightning rod coefficient, the longitudinal surface plasmon resonance frequency, and the spontaneous emission-resonator coupling factor for various eccentricity values. Calculations show a nonlinear increase in the lightning rod coefficient with increasing eccentricity. In the limiting case of an infinitely long (cylindrical) particle, the lightning rod coefficient is infinitely large.

The longitudinal surface plasmon resonance frequency values presented in the table indicate a decrease with increasing eccentricity. This is consistent with experimental data on the localization of longitudinal SPR frequencies of cylindrical particles in the visible or infrared spectral range.

The size dependences of the efficiency and the spontaneous emission rate change are shown in Fig. 4. Both the efficiency and the spontaneous emission rate change increase with increasing eccentricity. However, there is a significant difference between their size dependences. While the efficiency at any eccentricity is higher for larger spheroids (with longer semi-axes), the spontaneous emission rate change is always greater for smaller particles, which is due to the increase in the surface area to volume ratio with decreasing particle size.

Figure 5 shows the frequency and size dependence curves for the longitudinal component of the Q-tensor. Note that the longitudinal component of the Q-tensor increases monotonically in the infrared and visible spectral ranges, and for any frequency, it is greater with longer semi-axes and greater eccentricity.

The frequency and size dependences of the Purcell factor of a spheroidal nanoantenna-resonator are shown in Figure 6. The dependence $\mathcal{F}_p^{\parallel}(\hbar\omega)$ is similar to the dependence $\mathscr{G}_{\parallel}(\hbar\omega)$; the curves of these dependences have maxima at the same frequencies and the same shift of the maxima with increasing eccentricity. The behavior of the size dependences of the Purcell factor is similar to the behavior of the size dependences for the longitudinal components of the field enhancement and the quality factor, as expected based on the relationships linking these characteristics.

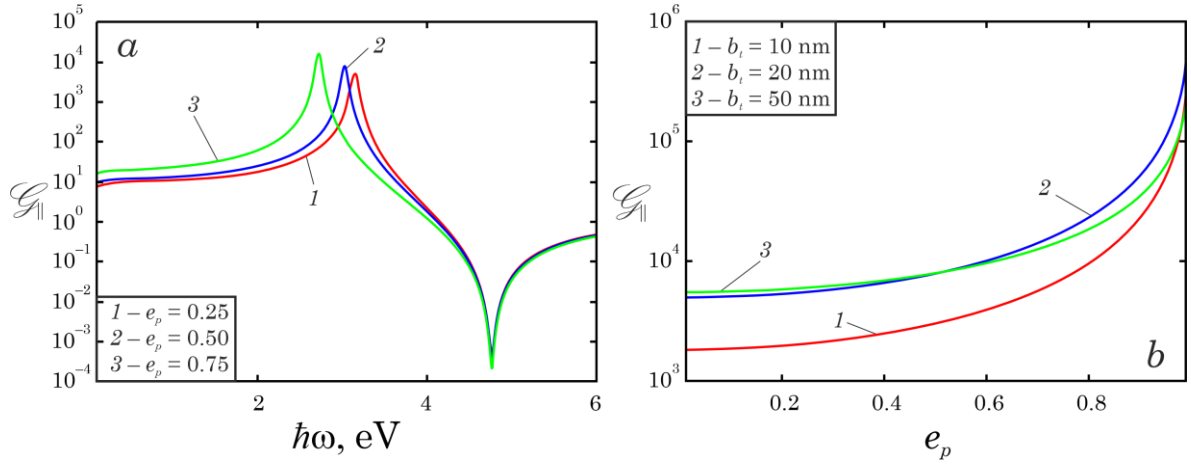

Fig. 3 – Frequency (*a*) and size (*b*) dependences of the longitudinal component of the electric field enhancement tensor for prolate spheroidal Ag nanoparticles.

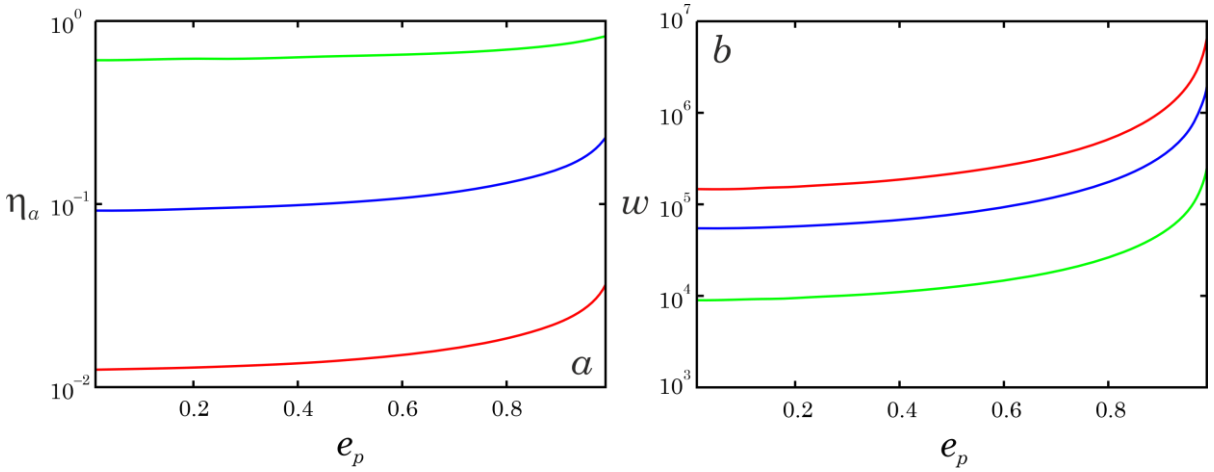

Fig. 4 – Size dependences of the efficiency (*a*) and the spontaneous emission rate change (*b*) for the same values b_t as in Fig. 3, *b*.

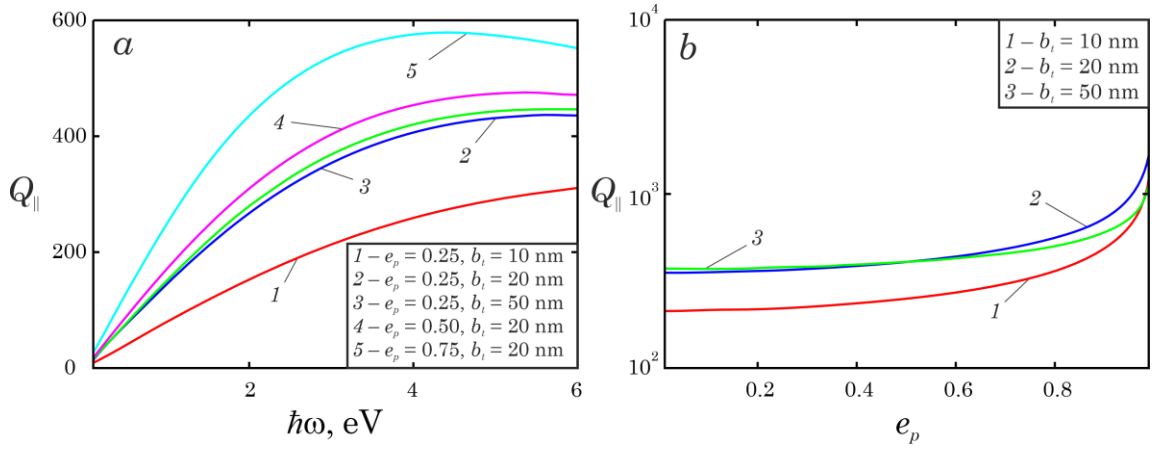

Fig. 5 – Frequency (*a*) and size (*b*) dependences of the longitudinal quality factor for prolate spheroidal Ag nanoparticles.

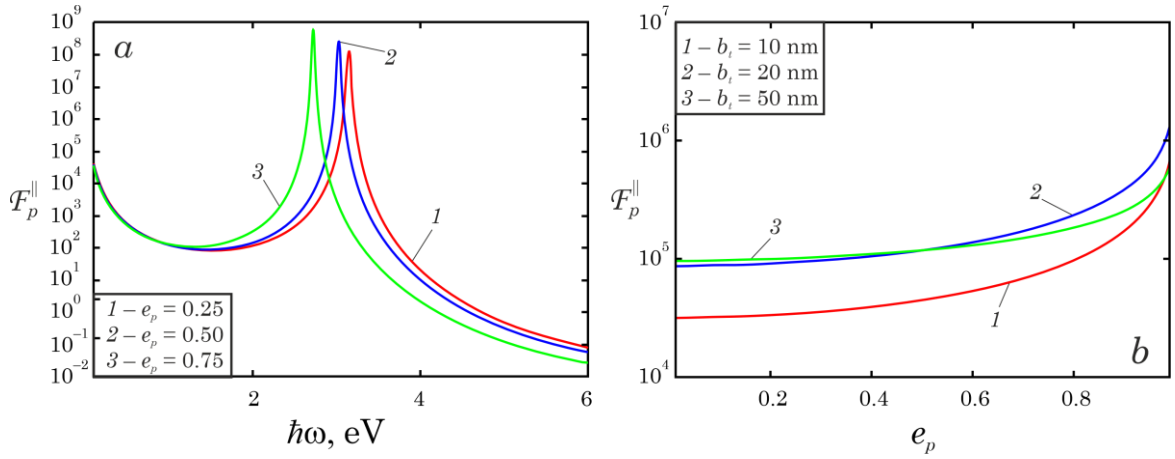

Fig. 6 – Frequency (*a*) and size (*b*) dependences of the longitudinal Purcell factor for prolate spheroidal Ag nanoparticles.

Table 2 presents the values of the spontaneous emission-resonator coupling factor for various eccentricities of the spheroidal resonator-particle. The $\beta_\parallel(e_p)$ calculation results indicate the presence of a strong coupling of spontaneous emission with the resonator ($\beta_\parallel \to 1$) in the infrared and visible spectral ranges. This fact confirms the hypothesis of a close relationship between the antenna and resonator properties of plasmonic nanoparticles.

4. CONCLUSIONS

Expressions for the frequency and size dependences of the antenna and resonator characteristics of metallic nanoparticles in the shape of an prolate spheroid were obtained, and relationships between these characteristics were established.

It has been demonstrated that with an increase in the eccentricity of nanoparticles, a "red" shift of the maxima of the electric field enhancement, quality factor, and Purcell factor longitudinal components occurs with a simultaneous increase in the height of the maxima.

It has been shown that increasing the eccentricity of a spheroidal particle results in a nonlinear increase in the lightning rod coefficient, reaching very high values as the particle shape approaches a long cylinder. Under these conditions, the longitudinal surface plasmon resonance frequency shifts into the infrared region, that is confirmed by experimental results for cylinders (highly elongated spheroids).

It was found that, for a given eccentricity, unlike the longitudinal quality factor and efficiency, which are greater for larger particles, the spontaneous emission rate change is always greater for smaller particles. This is explained by the fact that the surface area to volume ratio increases with decreasing particle size.

A close relationship between the antenna and resonator properties of prolate spheroidal metal nanoparticles has been proven. This is evidenced by the spontaneous emission-resonator coupling factor being close to unity in the infrared and visible spectral regions.

REFERENCES

1. *Plasmonics: Principles and Applications* (Ed. K.Y. Kim) (ITAe: 2012).
2. *Plasmonics: Theory and Applications* (Ed. T.V. Shahbazyan, M.I. Stockman) (Springer Dordrecht, 2013).
3. *Plasmonics and its Applications* (Ed. G. Barbillon) (Basel, Switzerland: MDPI: 2019).
4. A.O. Koval, A.V. Korotun, Yu.A. Kunytskyi, V.A. Tatarenko, I.M. Titov, *Electrodynamics of Plasmon Effects in Nanomaterials* (Kyiv: Naukova Dumka: 2021) [In Ukrainian].
5. H. Chen, H. Yun, M. Jiang, Q.-H. Wei, *J. Opt. Soc. Am. B*

41, 2661 (2024) https://doi.org/10.1364/JOSAB.543394.
6. N.I. Zheludev, *Nat. Mater.* **7**, 420 (2008) https://doi.org/10.1038/nmat2163.
7. M.S. Tame, K.R. McEnery, Ş.K. Özdemir, J. Lee, S.A. Maier, M.S. Kim, *Nat. Phys.* **9**, 329 (2013) https://doi.org/10.1038/nphys2615.
8. P.A. Crozier, M. Leibovich, P. Haluai, Y. Wang, C. Fernandez-Granda, *Science* **387**, 949 (2025) https://doi.org/10.1126/science.ads2688.
9. Z.-J. Yang, R.B. Jiang, X.L. Zhuo, Y.-M. Xie, J.F. Wang, H.-Q. Lin, *Phys. Rep.* **701**, 1 (2017) https://doi.org/10.1016/j.physrep.2017.07.006.
10. H. Yagi, S. Uda, *Proc. Imp. Acad. Jpn.* **2**, 49 (1926) https://doi.org/10.2183/pjab1912.2.49.
11. A.G. Curto, G. Volpe, T.H. Taminiau, M.P. Kreuzer, R. Quidant, N.F. van Hulst, *Science* **329**, 930 (2010) https://doi.org/10.1126/science.1191922.
12. T. Kosako, Y. Kadoya, H.F. Hofmann, *Nature Photon.* **4**, 312 (2010) https://doi.org/10.1038/nphoton.2010.34.
13. V. Giannini, A.I. Fernández-Domínguez, S.C. Heck, S.A. Maier, *Chem. Rev.* **111**, 3888 (2011) https://doi.org/10.1021/cr1002672.
14. Y. Li, N. Engheta, *Phys. Rev. Appl.* **10**, 054021 (2018) https://doi.org/10.1103/PhysRevApplied.10.054021.
15. J.H. Yang, Y.Z. Guo, W.Z. Lu, R.B. Jiang, J.F. Wang, *Adv. Mater.* **30**, 1802227 (2018) https://doi.org/10.1002/adma.201802227.
16. A.V. Korotun, D.V. Demianenko, V.I. Reva, R.A. Kulykovskyi, *Chem. Phys. Technol. Surf.* **16** No 2, 253 (2025) https://doi.org/10.15407/hftp16.02.253.
17. K. Saha, S.S. Agasti, C. Kim, X.N. Li, V.M. Rotello, *Chem. Rev.* **112**, 2739 (2012) https://doi.org/10.1021/cr2001178.
18. S. Linic, P. Christopher, D.B. Ingram, *Nat. Mater.* **10**, 911 (2011) https://doi.org/10.1038/nmat3151.
19. A.V. Korotun, S.I. Shylo, V.I. Reva, I.M. Titov, *J. Nano-Electron. Phys.* **17** No1, 01013 (2025) https://doi.org/10.21272/jnep.17(1).01013.
20. M. Kauranen, A.V. Zayats, *Nature Photon.* **6**, 737 (2012) https://doi.org/10.1038/nphoton.2012.244.
21. *Optical Antennas* (Ed. M. Agio, A. Alù) (Cambridge University Press: 2013).
22. K. Yao, Y.M. Liu, *ACS Photon.* **3**, 953 (2016) https://doi.org/10.1021/acsphotonics.5b00697.
23. X.M. Zhang, J.-J. Xiao, Q. Zhang, F.F. Qin, X.M. Cai, F. Ye, *ACS Omega* **2**, 774 (2017) https://doi.org/10.1021/acsomega.7b00121.
24. X.L. Zhuo, H.K. Yip, X.M. Cui, J.F. Wang, H.-Q. Lin, *Light: Sci. Appl.* **8**, 39 (2019) https://doi.org/10.1038/s41377-019-0150-1.
25. A. Ahmed, R. Gordon, *Nano Lett.* **12**, 2625 (2012) https://doi.org/10.1021/nl301029e.
26. M. Agio, *Nanoscale* **4**, 692 (2012) https://doi.org/10.1039/C1NR11116G.
27. A. Korotun, G. Moroz, R. Korolkov, I. Titov, *IEEE XIIIth International Conference on Electronics and Information Technologies (ELIT-2023)*, 320 (Lviv: 2023).
28. H.V. Moroz, V.P. Kurbatsky, A.V. Korotun, N.M. Nagorna, *J. Nano- Electron. Phys.* **16** No 6, 06032 (2024) https://doi.org/10.21272/jnep.16(6).06032.
29. D. Vercruysse, Y. Sonnefraud, N. Verellen, F.B. Fuchs, G.D. Martino, L. Lagae, V.V. Moshchalkov, S.A. Maier, P.V. Dorpe, *Nano Lett.* **13**, 3843 (2013) https://doi.org/10.1021/nl401877w.
30. Y.Y. Tanaka, T. Shimura, *Nano Lett.* **17**, 3165 (2017) https://doi.org/10.1021/acs.nanolett.7b00672.
31. X.L. Zhuo, H.K. Yip, Q.F. Ruan, T.K. Zhang, X.Z. Zhu, J.F. Wang, H.-Q. Lin, J.-B. Xu, Z. Yang, *ACS Nano* **12**, 1720 (2018) https://doi.org/10.1021/acsnano.7b08423.
32. R. Verre, M. Svedendahl, N.O. Länk, Z.J. Yang, G. Zengin, T.J. Antosiewicz, M. Käll, *Nano Lett.* **16**, 98 (2016) https://doi.org/10.1021/acs.nanolett.5b03026.
33. N.I. Pavlyshche, A.V. Korotun, V.P. Kurbatsky, *Him. Fiz. Tekhnol. Poverkhni.* **14** No4, 561 (2023).
34. A.V. Korotun, H.V. Moroz, R.Yu. Korolkov, *Funct. Mater.* **31** No1, 119 (2024) https://doi.org/10.15407/fm31.01.119.

Оптична антена-резонатор на основі металевої витягнутої сфероїдальної наночастинки

А.В. Коротун[1,2], В.П. Курбацький[1], Г.В. Мороз[1], Р.Ю. Корольков[1], Н.М. Нагорна[1]

[1] *Національний університет «Запорізька політехніка», 69063 Запоріжжя, Україна*
[2] *Інститут металофізики ім. Г. В. Курдюмова НАН України, 03142 Київ, Україна*

У роботі досліджено антенні та резонаторні характеристики витягнутих сфероїдальних металічних наночастинок. Обговорюється принцип роботи оптичної нанорозмірної антени. Встановлено зв'язок між антенними та резонаторними властивостями металевих наночастинок. Отримано частотні та розмірні залежності поздовжнього підсилення поля, добротності, фактора Парселла та фактора зв'язку спонтанного випромінювання з резонатором, а також розмірні залежності коефіцієнтів блискавковідводу, корисної дії, частоти поздовжнього поверхневого плазмонного резонансу та зміни швидкості спонтанної емісії. Встановлено співвідношення, що пов'язують зазначені величини одна з одною, які свідчать про наявність тісного зв'язку між характеристиками оптичних нанорозмірних антен і нанорезонаторів. Описано поведінку максимумів частотних залежностей поздовжнього підсилення поля та фактора Парселла за зміни ексцентриситету сфероїдальної наночастинки. Показано, що зі збільшенням ексцентриситету частинки (наближенням її форми до циліндричної) коефіцієнти блискавковідводу, корисної дії та зміни швидкості спонтанної емісії збільшуються. При цьому частота поздовжнього поверхневого плазмонного резонансу зменшується, переходячи з ближнього ультрафіолетового в оптичний (для частинок деяких металів – інфрачервоний) діапазон. Встановлено, що у граничному випадку частинки нескінченної довжини коефіцієнт блискавковідводу стає нескінченно великим. Виявлено тісний зв'язок між антенними та резонаторними властивостями сфероїдальних наночастинок, що підтверджується близькою до одиниці величиною фактора зв'язку спонтанного випромінювання з резонатором в інфрачервоній та видимій областях спектру. Встановлено, що зростання відношення площі поверхні до об'єму наночастинок при зменшенні їх розміру призводить до зменшення коефіцієнта корисної дії та збільшення зміни швидкості спонтанної емісії. Крім того, при збільшенні розмірів (довжин півосей) наночастинок спостерігається зростання поздовжньої компоненти тензора добротності.

Ключові слова: Оптична наноантена, Нанорезонатор, Коефіцієнти блискавковідводу та корисної дії, Підсилення електричних полів, Добротність, Фактор Парселла.